

Figure 10. (Ksapabutr et al.)

()

ภาคผนวก ข.3

Fabrication of gadolinium doped ceria thin film by electrostatic spray deposition equipped with external permanent magnets. (Submitted to *Thin Solid Films*)

Fabrication of gadolinium doped ceria thin film by electrostatic spray deposition equipped with external permanent magnets

Bussarin Ksapabutr^{a,*}, Manop Panapoy^a, Khongrat Tragolrat^a,
Sujitra Wongkasemjit^b

^a Department of Materials Science and Engineering, Faculty of Engineering and Industrial Technology, Silpakorn University, Sanamchandra Palace Campus, Nakhon Pathom 73000, Thailand.

^b The Petroleum and Petrochemical College, Chulalongkorn University,

Bangkok 10330, Thailand

Abstract

A cost-effective and promising simple deposition method, electrostatic spray deposition (ESD) was used to fabricate dense gadolinium doped ceria (GDC) thin films. The effect of the magnetic field on the deposition area of the emitted spray upon the substrate using two external permanent magnets, the morphology and microstructure of GDC films was investigated. The data showed that the coating area deposited by ESD-spray with two same magnetic poles of permanent magnets on the substrate decreased in comparison with the case of no external permanent magnet. On the other hand, the largest deposition area was presented using two opposite poles of permanent magnets during fabrication. Analysis of as-deposited films using SEM, AFM and XRD indicated the formation of the uniform, smooth and dense thin films with the single-phase fluorite structure. Additionally, the films produced with two

138

same pole magnets were thicker and smaller in crystallite size than those fabricated

under other conditions.

Keywords: Gadolinium doped ceria; Electrostatic spray deposition; Magnetic field;

Charged droplets

*Corresponding author. Tel.66-34-219-363; Fax.66-34-219-363;

E-mail address: bussarin@su.ac.th (B. Ksapabutr)

1. Introduction

Over the past two decades, there has been a significant growth of interest in

research and development in solid oxide fuel cells (SOFCs). They have emerged as a

leading technology to provide the clean and efficient power sources of the future. The

recent trend in the development of SOFCs is to decrease the operating temperature

below 900°C [1-3]. The attractive advantages of reduced-temperature operation for

the SOFCs are offered by a longer cell life, wider choice of materials, improved

reliability, reduced thermal stress, and reduced material and maintenance costs.

Another crucial benefit of reduced-temperature operation is the possibility of using

low-cost metals as the interconnect materials [4-5]. In general, two approaches are

extensively applied to reduce the resistance of electrolyte films, either by using the

alternative electrolytes with better oxygen ionic conductivity at lower operating

temperature or by decreasing the thickness of conventional YSZ-based SOFCs. So

far, doped ceria materials are being widely investigated as a promising candidate solid

electrolyte for intermediate temperature SOFCs (IT-SOFCs). These materials

demonstrate much higher ionic conductivity at relatively lower temperatures in

comparison with that of the traditional yttria-stabilized zirconia (YSZ) electrolyte [6-

10].

A variety of fabrication techniques, such as screen-printing, slurry coating, sol-gel, tape casting, and dry pressing, have been widely used to prepare films in both laboratory and industrial practices due to their simplicity, low-cost, and high productivity. To achieve better control on film quality, other techniques, mostly vapor processing approaches, such as physical vapor deposition (PVD) [11], chemical vapor deposition (CVD) [12], electrochemical vapor deposition (EVD) [13], thermal spray [14], metal-organic chemical vapor deposition (MOCVD) [15], sputtering [16], and flame assisted vapor deposition (FAVD) are presently available for fabrication of SOFC components [17]. Generally, these methods require special raw materials and targets, sophisticated equipment and well-controlled atmosphere, therefore increasing the capital investment and fabrication costs. Furthermore, the films fabricated by some of these approaches require post-deposition heat treatment, which is costly and time consuming.

Recently, another novel and cost-effective alternative thin-film forming approach is electrostatic spray deposition (ESD), in which a liquid flowing through a capillary nozzle can be subjected to a high voltage to produce a spray and move towards a grounded substrate, upon which it ultimately deposits and builds up a solid layer. This method has several advantages over conventional deposition techniques, such as no usage of sophisticated reactor, non-vacuum deposition condition, inexpensive and non-toxic precursors, easy control of substrate temperature, and defect reparation [18-20]. However, the area of the deposition cannot be easily controlled. To our knowledge, thin films have not been fabricated with ESD technique assembled with external permanent magnets so far.

The aim of the present work is to elucidate the influence of magnetic field arising from external permanent magnets on the deposition area and the morphology

of GDC thin films prepared by ESD technique. Moreover, the use of electrostatic spray deposition with external permanent magnets to fabricate dense and crack-free GDC thin films was also investigated.

2. Experimental

2.1 ESD setup

A schematic diagram of the equipment used in this work for ESD was shown in Fig. 1(a). This system is composed mainly of three parts: (1) an electrostatic spray unit, including a high DC voltage power supply and a stainless steel nozzle (0.394 mm inner diameter and 0.711 mm outer diameter) with a tilted tip of 15° at the end; (2) a liquid feeding unit, including a syringe pump and a liquid container; (3) a temperature control unit, including a temperature controller and a heating element. A DC voltage of 15 kV was applied between a nozzle (THD Ltd. No.22) and a stainless steel (316L) substrate. Precursor solution was emitted at the orifice of the nozzle and consequently, a spray was deposited as a thin layer on the substrate.

2.2 Effect of external permanent magnets on deposition

2.2.1 Deposition area of coverage

A precursor solution with Gd:Ce mole ratio of 0.1:0.9, stoichiometric amounts of gadolinium nitrate hexahydrate (Gd(NO₃)₃.6H₂O, 99.99 % purity, Aldrich Chemical) and cerium nitrate hexahydrate (Ce(NO₃)₃.6H₂O, 99.99 % purity, Aldrich Chemical) dissolved in ethanol (C₂H₅OH, 99 % purity, Fluka) at total concentration of 0.01 mol dm⁻³, was pumped toward the nozzle at a flow rate of 1 ml h⁻¹. The substrate temperature, the deposition time, and the nozzle-to-substrate distance were set at 100°C, 2 h, and 9 cm, respectively. To evaluate the influence of the external magnetic

field on the deposition area, the spraying was operated under both conditions with and without permanent magnets. Two external permanent magnets having magnetic induction intensity (B) of 250 Gauss were placed 6 cm above the substrate. Two arrangements of magnet position, same and opposite magnetic poles, were located, as illustrated in Fig. 1(b). The distance of 8 cm was kept between two external magnets.

2.2.2 Fabrication of GDC films using ESD without and with external permanent magnets

The same precursor solution used in section (2.2.1) was fed into the nozzle at the flow rate of 1 ml h⁻¹. For each deposition, the distance between the nozzle and the substrate was 9 cm, while the deposition time was 2 h. The deposition temperature was controlled at 450°C. To investigate the influence of external magnetic field on the morphology of thin films, the same arrangements of magnet position employed in section (2.2.1) were also established.

2.3 Characterization

Thermogravimetric analysis (TGA) was performed using a TGA7 Perkin-Elmer thermal analysis system with a scanning rate of 5°C min⁻¹. The as-deposited films were characterized using a scanning electron microscope (SEM, Cam Scan, Maxim 2000S) with an energy dispersive X-ray (EDX) microanalyzer for the observation of surface morphology and chemical composition. The structure features were obtained by X-ray diffractometer (XRD, Model Rigaku D/Max 2000HV) with monochromatic Cu K α radiation (λ = 1.542 Å). The transmission electron microscopy (TEM) analysis was carried out using a JEOL JEM-2010 electron microscope with a filament of LaB₆. The system was operated at 200 kV with a point resolution of 0.23

nm. The samples were placed on carbon film supported on a copper grid by applying a few droplets of ground sample with ethanol and then dried in air. The film thickness was attained from scanning electron microscope (SEM, Hitachi, S3400N) for films deposited on glass substrate. The roughness of the films was revealed by an atomic force microscope (AFM, Seiko, SPI 400 DFM mode). Magnetic field was measured using Hall-effect sensor (No.A1302).

3. Results and discussion

Fig. 2 exhibits the photographs of the GDC coating using ESD technique, with and without permanent magnets. Deposition area coverage decreased when two permanent magnets were placed in the manner of the same magnetic poles (northnorth, or south-south) in comparison with the condition of no external permanent magnet. On the contrary, with the arrangement of the permanent magnets in the opposite poles, the deposition area coverage was greater. The quantitative deposition area on the substrate can be computed using Simpson's rule [21]. From the calculation, the deposition areas were 442.27, 216.74 and 607.11 mm² for the conditions of no magnet, same pole and opposite pole, respectively. The deposition area for the condition under the same poles was approximately 2 times lower than that under no magnet. With coating under the opposite poles, the area was approximately 1.4 times larger than that obtained in case of no magnet. It can be justified that at the substrate, the different arrangements of two permanent magnets leads to the different magnetic fields, as demonstrated in Fig. 3. The center position (at y = 0 and x = 0) between two same pole magnets provided the highest magnetic induction intensity (B). For the opposite pole arrangement, the highest magnetic induction intensity was shown at x = -2 and x = 2. In the case of the plasma system, the region of high

magnetic induction intensity results in high ion current density [22]. For the ESD system, liquid feeding is forced through a nozzle, which is maintained at an electric field with respect to a grounded plate, and atomized into small droplets. The resulting droplets are highly charged [23]. Therefore, charged droplets are considered instead of ions. It can be said that the center position between two same pole magnets results in the highest amount of charged droplets, leading to the smallest deposition area (see in Fig. 3(a)). In contrast, two magnets with the opposite pole pattern provided the highest charged droplet at the left and right sides from the center position between two magnets, which resulted in the largest deposition area, as displayed in Fig. 3(b).

In order to find out an appropriate deposition temperature for this investigation, GDC precursor solution was studied using TGA analysis. TG-DTG thermograms illustrated in Fig. 4 represent that major weight loss of the precursor solution occurred before 300°C was assigned to the evaporation of solvent and water, and the decomposition of nitrate [24]. Thus, the deposition temperature for the fabrication of GDC thin films in this work was controlled at 450°C.

The elemental compositions of all GDC thin films deposited under the condition of no magnet, same pole and opposite pole were justified using EDX analysis. At least fifteen points on all observed films were measured and the average values were exhibited. The observed Gd:Ce atomic ratio of all GDC thin films was approximately 0.12:0.88, which is in a good agreement with that of the starting solution (0.10:0.90).

The XRD patterns of all GDC thin films deposited at 450°C under the condition of no magnet, same pole, and opposite pole were demonstrated in Fig. 5. It was found that as-deposited films showed single phase crystallite with cubic fluorite structure. All films have a preferred growth orientation of (1 1 1). According to the

Debye-Scherrer's formula [25], the arithmetic mean crystallite sizes are 8.1, 5.8, and 6.8 nm for the condition of no magnet, same pole, and opposite pole, respectively. It can be observed that ESD-coating without external permanent magnet allows slightly better crystallization than those with opposite and same pole magnets, respectively. These observations were consistent with the TEM analysis. TEM micrographs of GDC films were shown in Fig. 6. Discontinuous ring of electron diffraction pattern was an evidence that the corresponding coating exhibited an insignificantly larger grain size, compared to other textured films where slightly more continuous rings were observed. As described in next paragraph, it is probably because the faster movement of charged droplets was accelerated by Lorentz and Coulombic forces under same pole magnets, leading to lower solvent evaporation compared to those under opposite pole magnets and no magnet, respectively. Hou et al. [26] also reported that the evaporation of solvent affected the nucleation and the subsequent growth of the film.

The SEM micrographs of GDC thin films deposited at 450°C, with and without permanent magnets were shown in Fig. 7. The dense microstructures with free of cracks were attained for all conditions. Nevertheless, the film prepared without permanent magnet showed higher agglomerates than those obtained using permanent magnets. With the arrangement of the permanent magnets in the same poles, the particle agglomeration was lower compared to that in the opposite poles. From the SEM pictures it is possible to determine the change in agglomerate density. The number of agglomerates per unit area was approximately 42.11 x 10⁻³, 7.33 x 10⁻³ and 22.67 x 10⁻³ µm⁻² for the conditions of no magnet, same pole and opposite pole, respectively. The values obtained were presented as arithmetic means of at least fifteen micrographs on five specimens. That might be because, in the condition of no

permanent magnet, the feeding liquid was atomized under an electric field from an orifice of nozzle, leading to the formation of the charged droplets or particles moving to the substrate by Coulombic force. Whereas magnetic force (Lorentz force) was negligible [27]. With using external permanent magnets, Lorentz force also affected charged droplets. The movement of the charged droplets in magnetic field resulted in the formation of Lorentz force perpendicular to the direction of the movement. The charged droplets had higher movement force, which resulted in the faster movement of the charged droplets to the substrate. Therefore, the surface morphology of GDC films deposited with and without permanent magnets might be determined by the speed of the charged droplets and the interactions between the precursor droplets and the heated substrate. Coincidently, Lu et al. [28] showed the numerical analysis of the fluid dynamics. The impact of the charged droplets resulted in the spreading at the substrate. For the deposition temperature of 100°C, the particle-like agglomerate morphology was revealed. However, in our experiment, the substrate temperature was controlled at 450°C. The evaporation of the solvent by the heat transfer from the heated substrate to the droplets should be completely occurred before the spreading of the droplet, leading to the agglomerate morphology. Interestingly, in our studies, the film deposited at 450°C with the arrangement of permanent magnets in the same poles exhibited relatively low agglomeration. This is most likely due to higher speed of the charged droplets in the presence of the permanent magnets in comparison with the circumstance of no permanent magnet, which resulted in lower solvent evaporation. Fig. 8 shows the magnetic induction intensity as a function of nozzle-to-substrate distance. As can be seen, the arrangement of the permanent magnets in the same poles has higher magnetic induction intensity than that in the opposite poles, which lead to lesser agglomeration, as described above.

The cross-sectional SEM images of the films deposited with and without permanent magnets (Fig. 9) reveal the dense and crack-free microstructures according to the top-view SEM micrographs (Fig. 7). With using two same pole magnets, GDC films showed the largest thickness compared to those deposited without magnet and with the opposite pole manner, respectively. This is because the center position between two same pole magnets had the highest amount of charged droplets. Whereas, the highest charged droplets were found at the side from the center position between two opposite pole magnets. This observation was also consistent with the results of the quantitative deposition area and 3D mapping.

Fig. 10 shows AFM images of the surface topology of thin films deposited with and without permanent magnets. Root mean square (RMS) roughnesses of the films were 22.78, 13.08, and 19.23 nm for the conditions of no magnets, same pole, and opposite pole, respectively. Apparently, the ESD-deposited film with permanent magnets in the same poles was smoothest. These observations were in agreement with the top-view SEM results. These results indicated that ESD technique assembled with external permanent magnets in the same poles is optimal for the fabrication of dense, uniform, smooth and crack-free GDC thin films. In forthcoming papers, the studies on other electrical properties of the thin films will be discussed in detail.

4. Conclusions

Nanocrystalline GDC thin films with dense microstructure and free of cracks have been successfully deposited using ESD technique coupled with external permanent magnets. The external magnetic field affected the area deposition coverage, the morphology and the crystallite size of the films. On the contrary, the chemical composition of GDC films did not depend on the external magnetic field.

Additionally, the arrangement of permanent magnets was also important. The use of an electrostatic and magnetic fields attracted the precursor solution to the substrate. Consequently, this minimized the loss of precursor to the surroundings and enhanced the deposition efficiency, as compared to ESD-coating without external permanent magnets. The ESD spray with two same pole magnets resulted in the highest uniformity and smoothness of dense coating with the thickness of approximately 1.6 µm.

5. Acknowledgements

The authors gratefully acknowledge the financial support received from the Thailand Research Fund (TRF), The Commission of Higher Education, Department of Materials Science and Engineering, Faculty of Engineering and Industrial Technology, Silpakorn University.

6. References

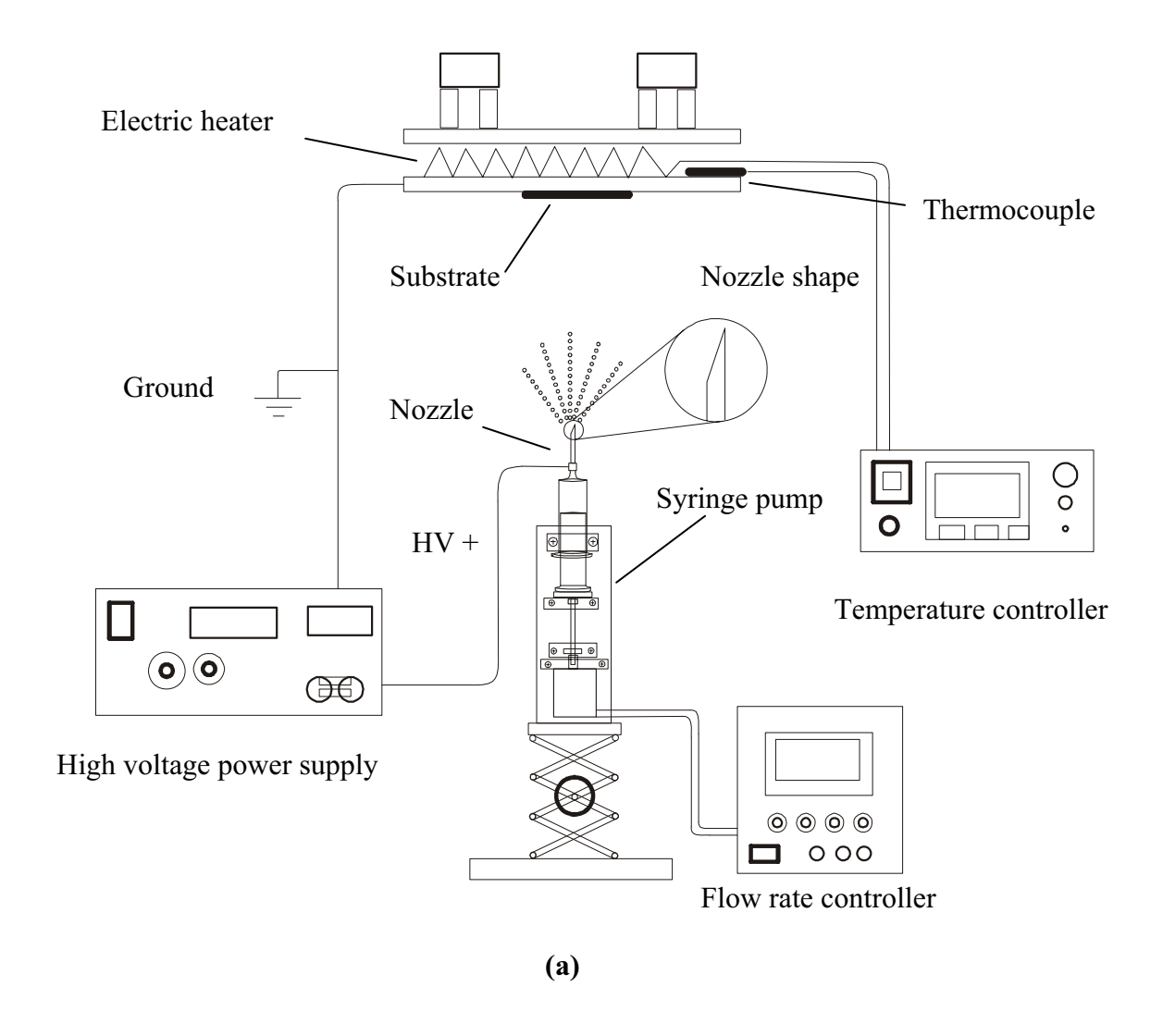
- J. Will, A. Mitterdorfer, C. Kleinlogel, D. Perednis, L.J. Gauckler, Solid State Ionics 131 (2000) 79.
- 2. S. Zha, C. Xia, X. Fang, H. Wang, D. Peng, G. Meng, Ceram. Int. 27 (2001) 649.
- 3. W. Bao, W. Zhu, G. Zhu, J. Gao, G. Meng, Solid State Ionics 176 (2005) 669.
- 4. S. Ohara, R. Maric, X. Zhang, K. Mukai, T. Fukui, H. Yoshida, T. Inagaki, K. Miura, J. Power Sources 86 (2000) 455.
- 5. L. Jian, J. Hueso, D. G. Ivey, J. Power Sources. 123 (2003) 151.
- 6. W. Huang, P. Shuk, M. Greenblatt, Solid State Ionics 100 (1997) 23.
- B. Zhu, X. T. Yang, J. Xu, Z. G. Zhu, S. J. Ji, M. T. Sun, J. C. Sun, J. Power Sources 118 (2003) 47.
- 8. J. G. Li, T. Ikegami, T. Mori, Acta Mater. 52 (2004) 2221.

- 9. E. Suda, B. Pacaud, M. Mori, J. Alloy. Compd. 408-412 (2006) 1161.
- H. H Huang, H. P. Chang, Y. T. Chien, M. C.Huang, J. S. Wang, J. Cryst. Growth 287 (2006) 458.
- 11. O. Unal, T.E. Mitchell, A.H. Heuer, J. Am. Ceram. Soc. 77 (1994) 984.
- 12. Y.B. Kim, S.G. Yoon, H.G. Kim, J. Electrochem. Soc. 139 (1992) 2559.
- 13. U.B. Pal, S.C. Singhal, J. Electrochem. Soc. 137 (1990) 2937.
- 14. A.R. Nicoll, A. Salito, K. Honegger, Solid State Ionics 52 (1992) 269.
- 15. Kueir-Weei Chour, Jong Chen, Ren Xu, Thin Solid Films 304 (1997) 106.
- P. K. Srivastava, T. Quach, Y. Y. Duan, R. Donelson, S. P. Jiang, F. T. Ciacchi, S.
 P. S. Badwal, Solid State Ionics 99 (1997) 311.
- S. Charojrochkul, R. M. Lothian, K. L. Choy, B. C. H. Steele, J. Eur. Ceram. Soc. 24 (2004) 2527.
- 18. T. Nguyen, E. Djurado, Solid State Ionics 138 (2001) 191.
- 19. I. Taniguchi, R. C. Van Landschoot, J. Schoonman, Solid State Ionics 160 (2003) 271.
- 20. C.-Y. Fu, C.-L. Chang, C.-S. Hsu, B.-H. Hwang, Mater. Chem. Phys. 91 (2005) 28.
- 21. S.C. Chapra, R.P. Canale, Numerical Methods for Engineers with Programming and Software Applications, McGraw-Hill, Singapore, 1998, p. 598.
- A.J. van Roosmalen, J.A.G. Baggerman, S.J.H. Brader, Dry Etching for VLSI, Plenum Press, New York, 1991, p. 94.
- A.G. Bailey, Electrostatic Spraying Liquids, Research Studies Press, England, 1988, p. 18.
- 3. M. Kamruddin, P.K. Ajikumar, R. Nithya, G. Mangamma, A.K. Tyagi, B. Raj, Powder Technol. 161 (2006) 145.

- 4. B.D. Cullity, Elements of X-Ray Diffraction, Addison–Wesley Publication Company, Reading, MA, 1978.
- 5. X. Hou, K.L. Choy, Surf. Coat. Technol. 180/181 (2004) 15.
- 6. S.E. Law, J. Electrostat. 51-52 (2001) 25.
- 7. J. Lu, J. Chu, W. Huang, Z.Ping, Sensors and Actuators A 108 (2003) 2.

Figure Captions

- **Figure 1.** (a) schematic view of ESD setup, (b) the arrangement of two permanent magnets
- **Figure 2.** Photographs of deposition distribution at the substrate temperature of 100°C with (a) no magnet; (b) same pole magnets; (c) opposite pole magnets.
- **Figure 3.** 3D maps of magnetic induction intensity at a given area (a) same pole magnets; (b) opposite pole magnets.
- **Figure 4.** TG-DTG thermograms of GDC precursor solution.
- **Figure 5.** XRD patterns of as-deposited GDC films at 450°C under (a) no magnet; (b) same pole magnets; (c) opposite pole magnets.
- **Figure 6.** TEM photographs of GDC coatings deposited at 450°C under (a) and (b) no magnet; (c) and (d) same pole magnets; (e) and (f) opposite pole magnets. Inset is the selected area electron diffraction (SAED) pattern.
- **Figure 7.** SEM micrographs of the GDC films deposited with (a) no magnet; (b) same pole magnets; (c) opposite pole magnets.
- **Figure 8.** Magnetic induction intensity as a function of nozzle-to-substrate distance
- **Figure 9.** SEM cross-sectional images of the GDC films deposited with (a) no magnet; (b) same pole magnets; (c) opposite pole magnets.
- **Figure 10.** AFM images of the GDC thin films fabricated under (a) no magnet; (b) same pole magnets; (c) opposite pole magnets.



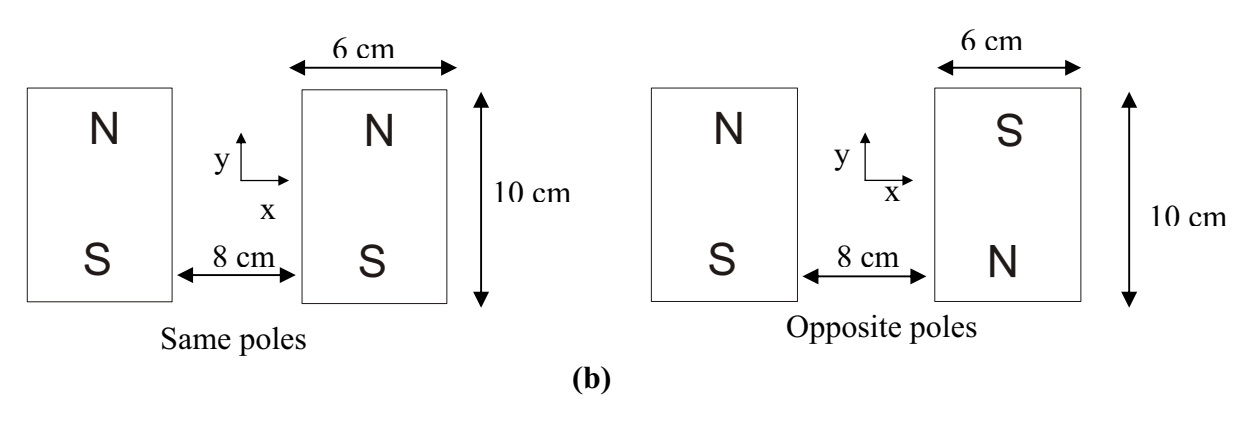


Figure 1. (Ksapabutr et al.)

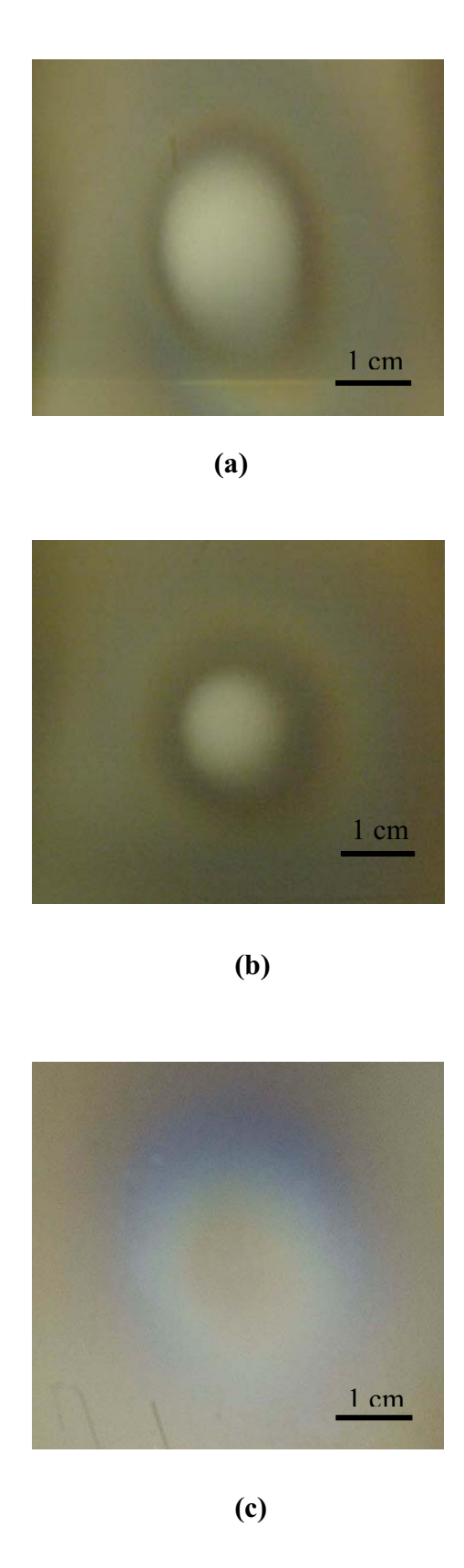
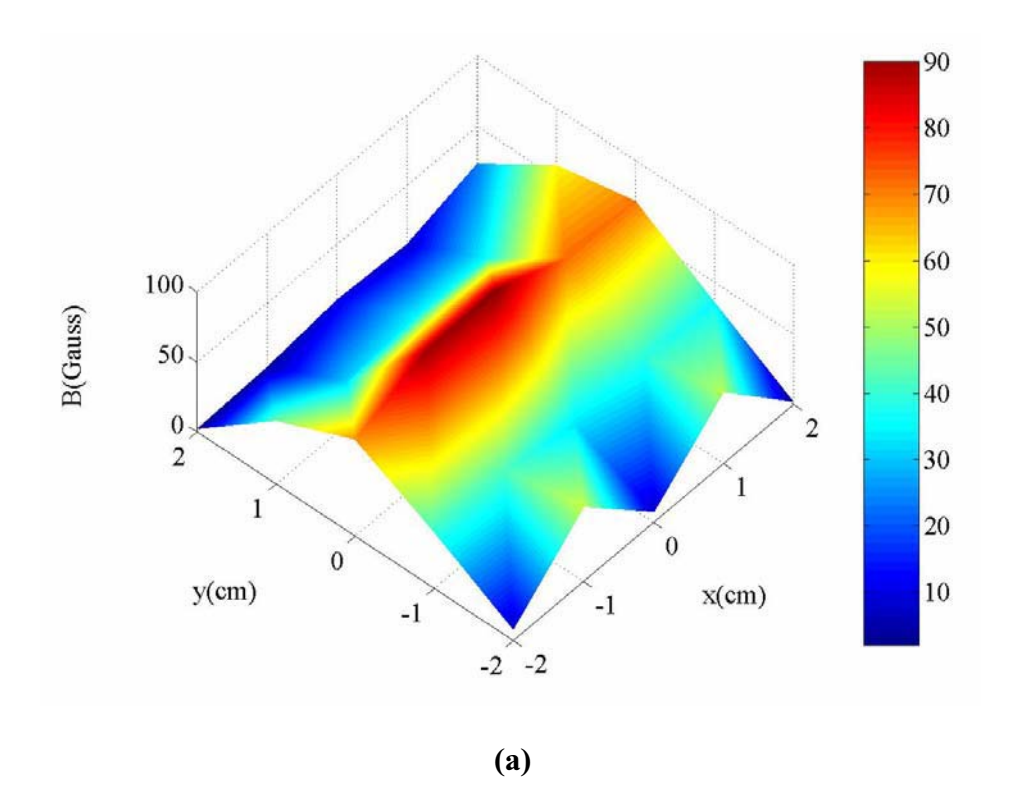


Figure 2. (Ksapabutr et al.)



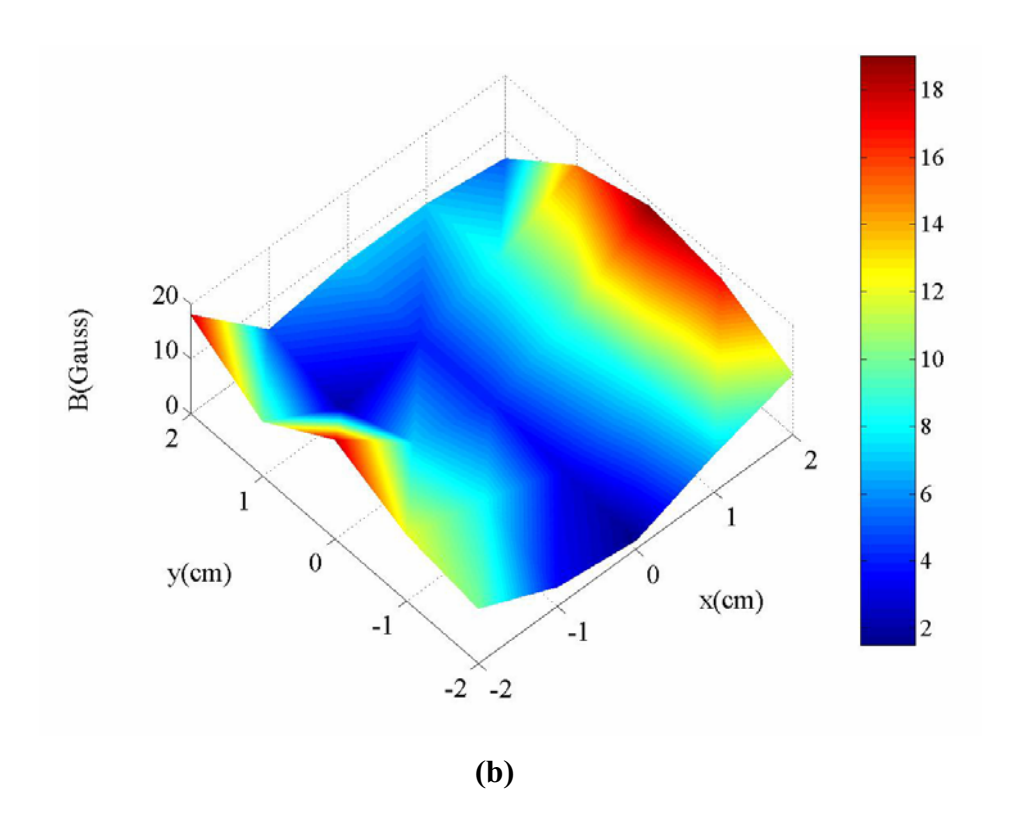


Figure 3. (Ksapabutr et al.)

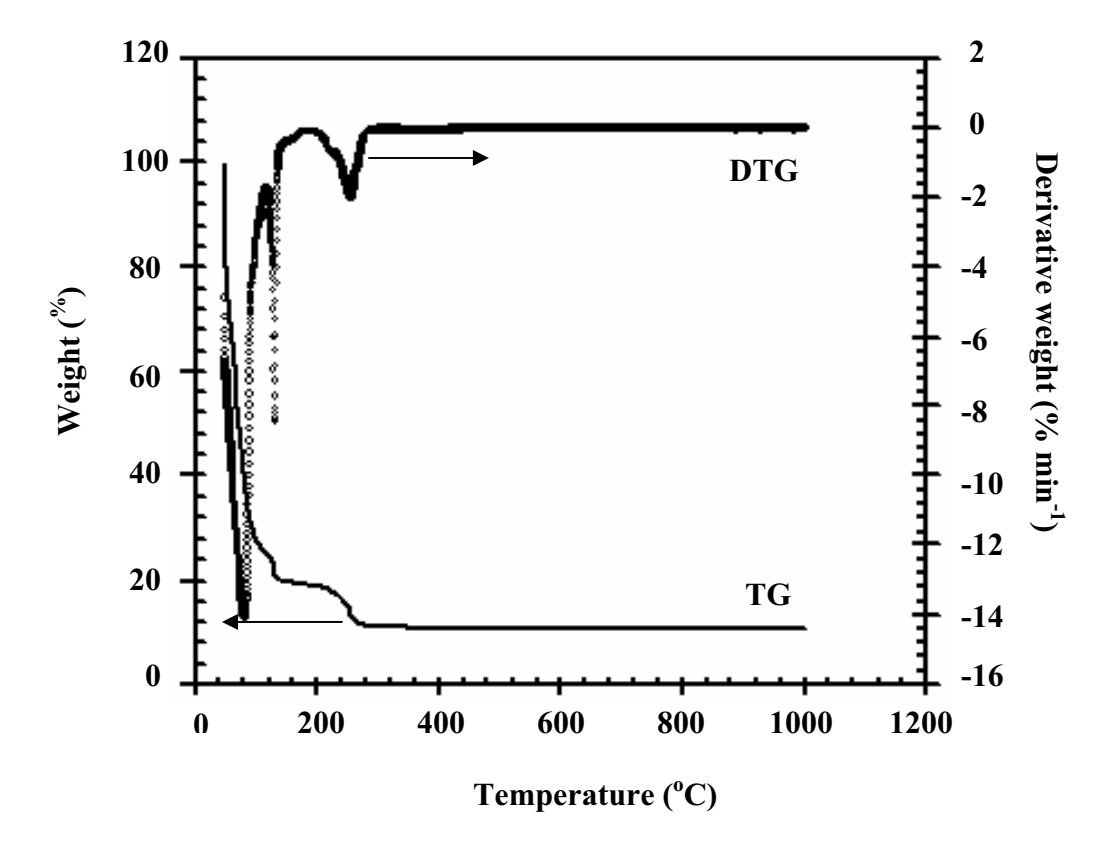


Figure 4. (Ksapabutr et al.)

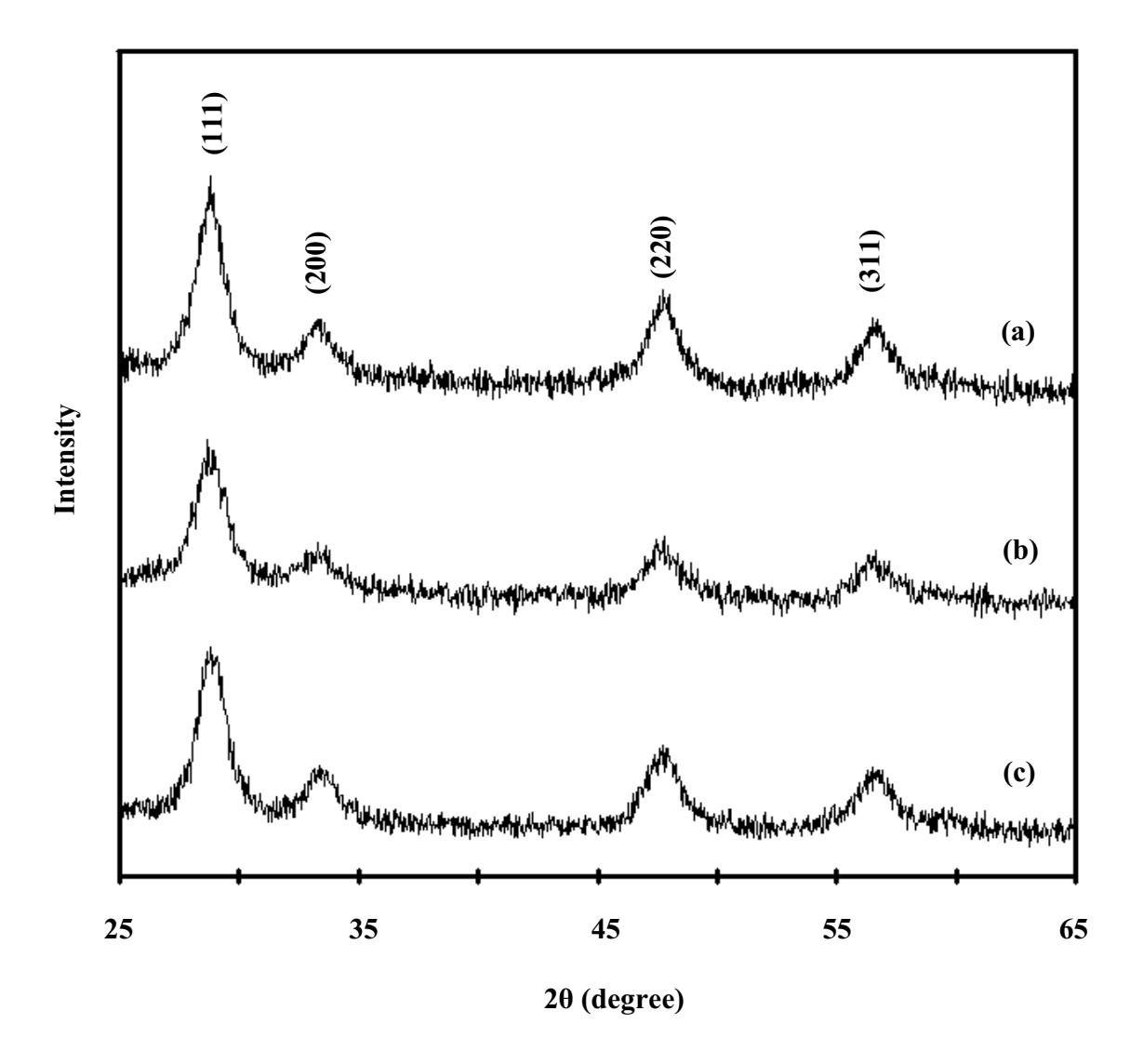


Figure 5. (Ksapabutr et al.)

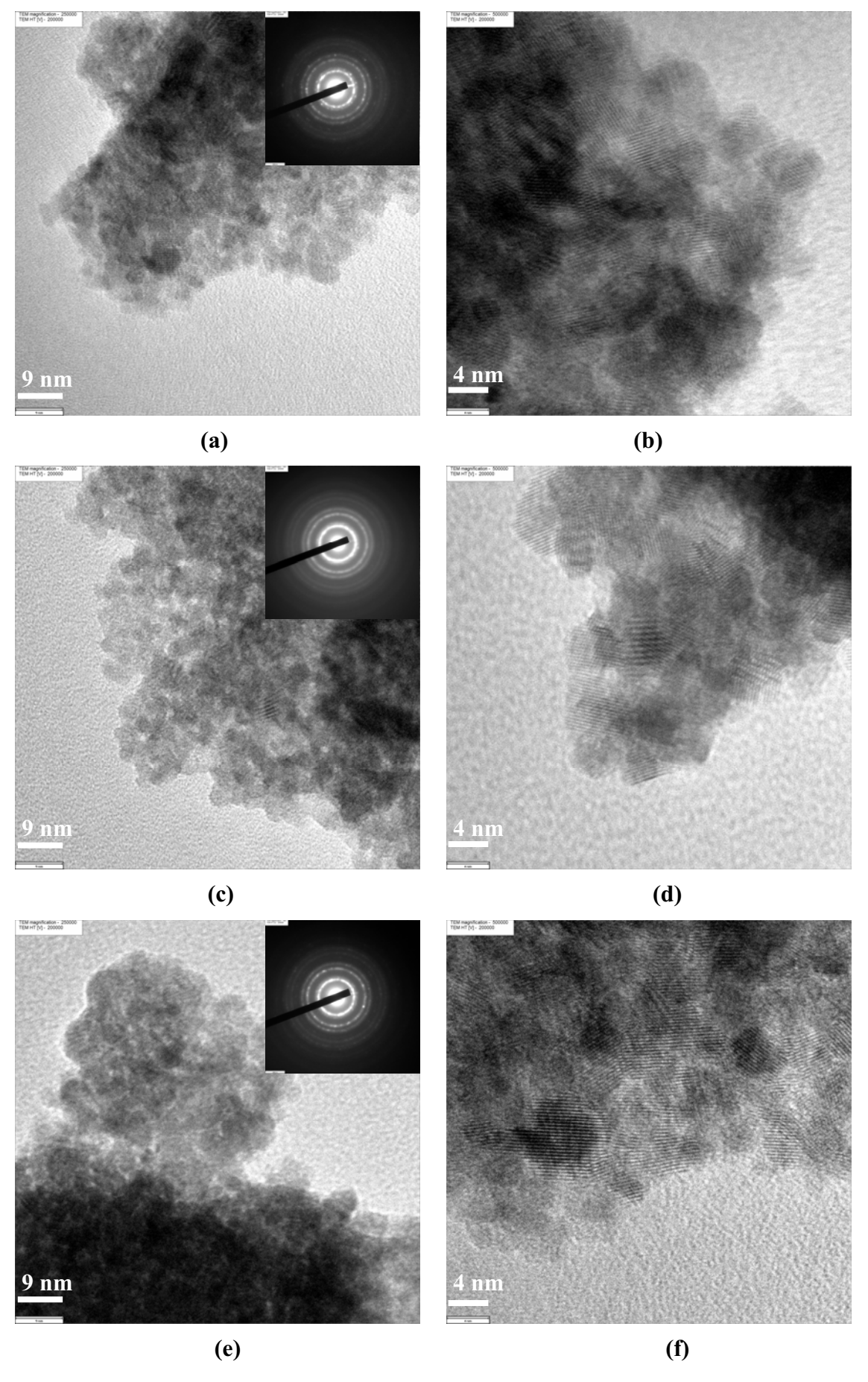
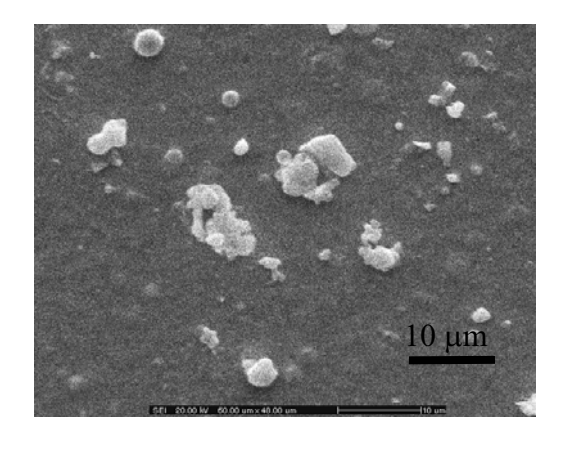
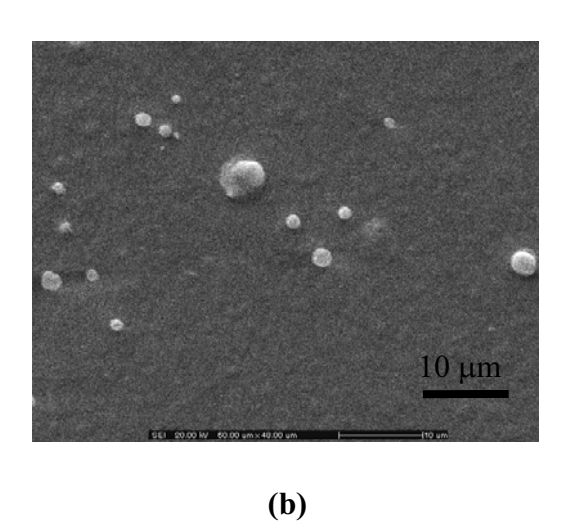


Figure 6. (Ksapabutr et al.)



(a)



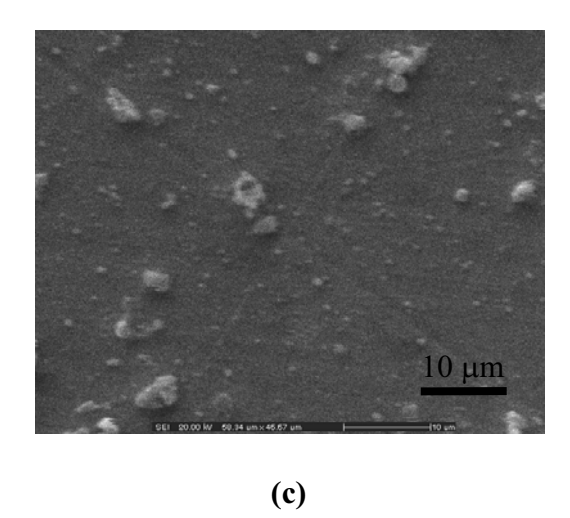


Figure 7. (Ksapabutr et al.)

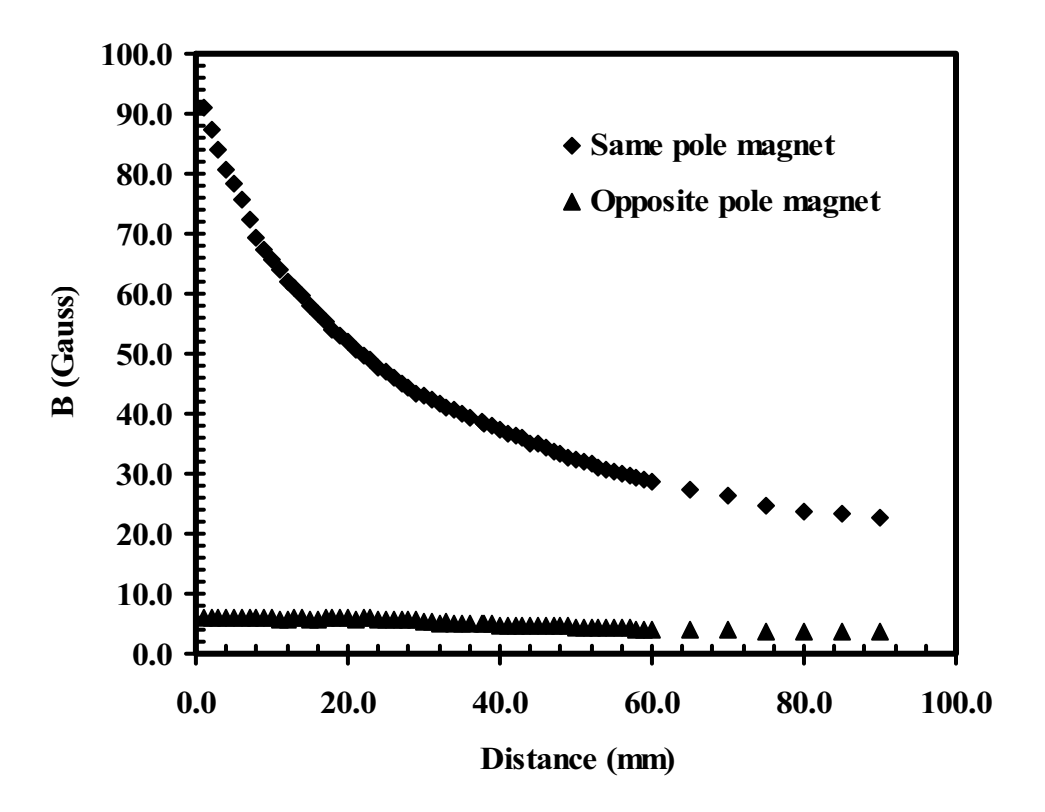
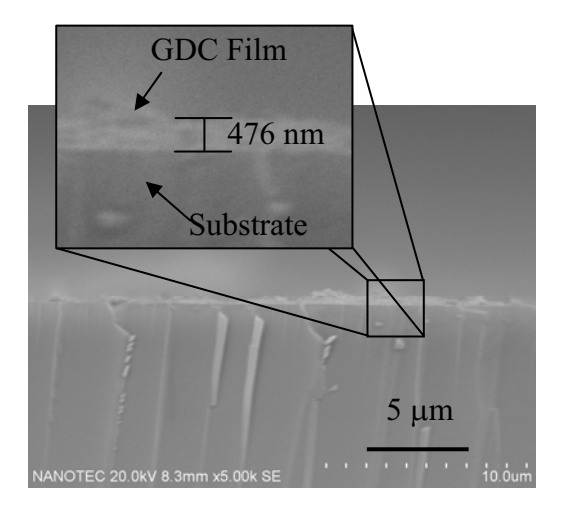
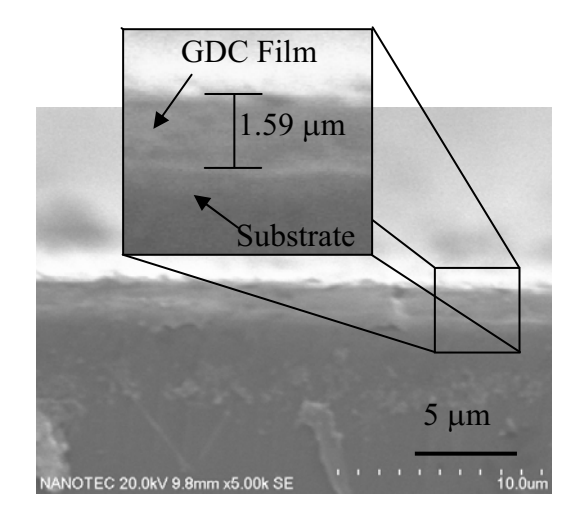


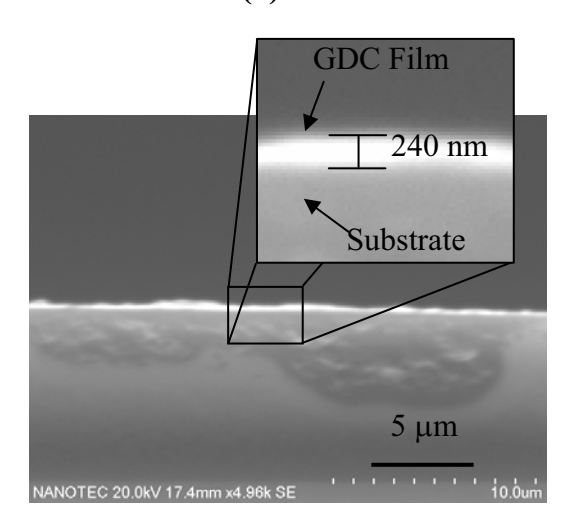
Figure 8. (Ksapabutr et al.)



(a)



(b)



(c)

Figure 9. (Ksapabutr et al.)

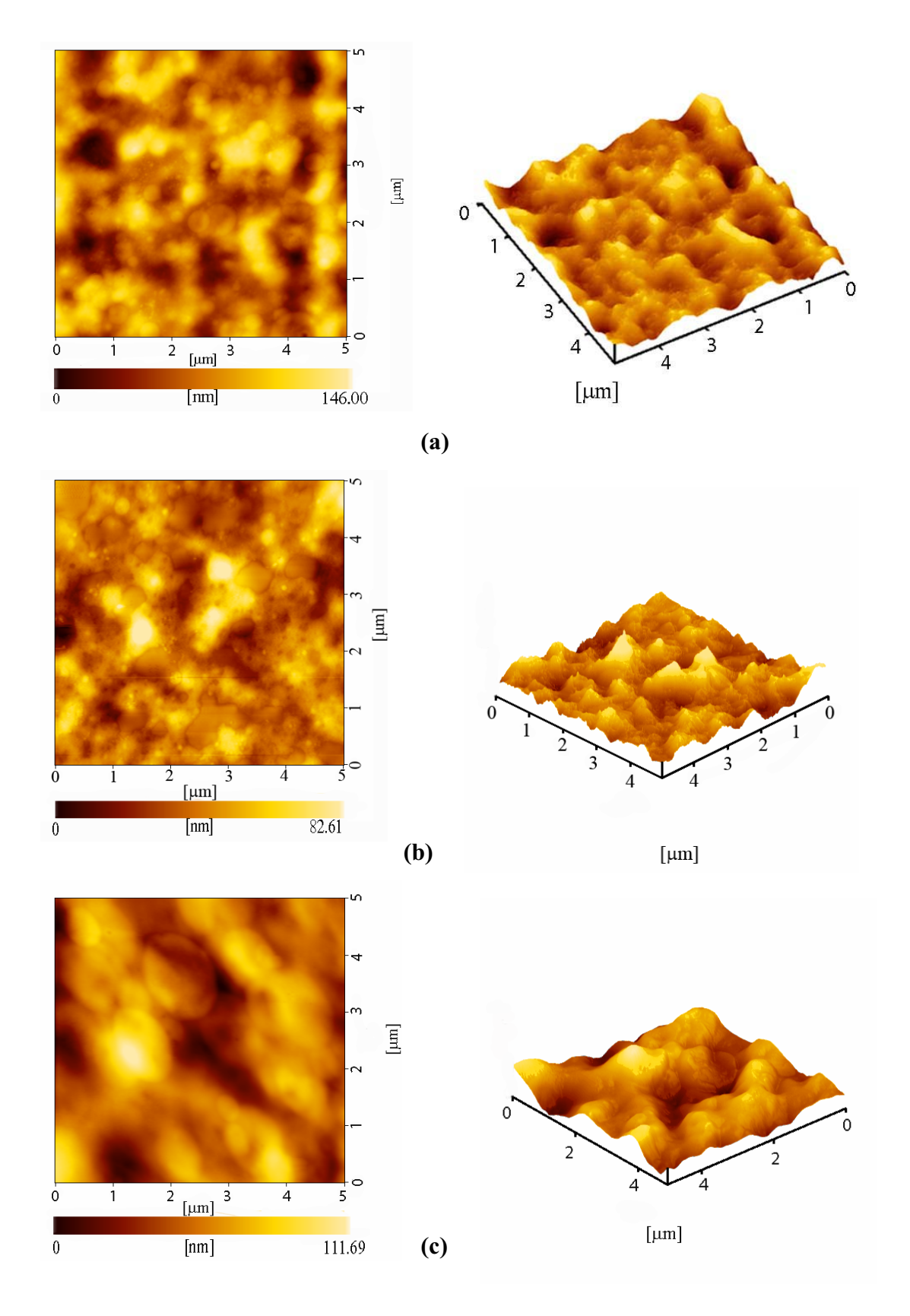


Figure 10. (Ksapabutr et al.)

ภาคผนวก ค.1

Abstract of International Meeting on Developments in Materials, Processes and
Applications of Nanotechnology (MPA-2007),
University of Ulster in Belfast, UK
(Poster Presentation)

Effect of Deposition Conditions on Morphology of Gadolinium Doped Ceria

Thin Film Coated by Electrostatic Spray Deposition Technique

Bussarin Ksapabutr^a*, Chaowat Waikru^a, Sujitra Wongkasemjit^b,

Manop Panapoy^a

^a Department of Materials Science and Engineering,

Faculty of Engineering and Industrial Technology, Silpakorn University,

Sanamchandra Palace, Nakorn Pathom 73000, Thailand

^b The Petroleum and Petrochemical College, Chulalongkorn University,

Bangkok 10330, Thailand

Gadolinium doped ceria thin film (GDC) was deposited on substrate in open

atmosphere using the cost-effective and simple coating technique referred to as

electrostatic spray deposition (ESD). The effect of deposition parameters, such as

substrate temperature, nozzle-to-substrate distance and liquid flow rate, on the surface

morphology and microstructure of thin films was examined with SEM, AFM and

XRD techniques. Thin films obtained became smooth and dense with increasing the

substrate temperature and the distance between the nozzle and substrate.

*Corresponding author. Tel.66-34-219-363; Fax.66-34-219-363;

E-mail address: bussarin@su.ac.th (B. Ksapabutr)

ภาคผนวก ค.2

Abstract of International Meeting on Developments in Materials, Processes and
Applications of Nanotechnology (MPA-2007),
University of Ulster in Belfast, UK
(Poster Presentation)

164

Electrostatic Spray Deposition of Samarium Doped Ceria Thin Film

Tanapol Chalermkiti, Bussarin Ksapabutr, Manop Panapoy*

Department of Materials Science and Engineering,

Faculty of Engineering and Industrial Technology, Silpakorn University,

Sanamchandra Palace, Nakorn Pathom 73000, Thailand

Abstract

Samarium doped ceria thin films were deposited on stainless steel substrate

using electrostatic spray deposition technique. The chemical analysis of the resulting

thin films was investigated by energy dispersive X-ray spectroscopy. The observed

chemical compositions of the films were in agreement with those of the starting

solutions. To achieve the dense thin films, the mixture solution of cerium nitrate and

samarium nitrate in ethanol or mixed solvent of ethanol and butylcarbitol was

employed.

*Corresponding author. Tel.66-34-219-363; Fax.66-34-219-363;

E-mail address: bussarin@su.ac.th (B. Ksapabutr)

ภาคผนวก ค.3

Abstract of The 3rd International Conference on Technological Advances of
Thin Films & Surface Coatings,
11th-15th December 2006
Grand Copthrone Waterfront Hotel, Singapore

(Oral Presentation)

หน้านี้เป็นเอกสารถ่ายเอกสาร

ภาคผนวก ค.4

Abstract of The 3rd International Conference on Technological Advances of

Thin Films & Surface Coatings,

11th-15th December 2006

Grand Copthrone Waterfront Hotel, Singapore

(Oral Presentation)

หน้านี้เป็นเอกสารถ่ายเอกสาร

หน้านี้เป็นเอกสารถ่ายเอกสาร